Geoscience Frontiers 9 (2018) 403–414

HOSTED BY

Contents lists available at ScienceDirect

China University of Geosciences (Beijing)

Geoscience Frontiers

journal homepage: www.elsevier.com/locate/gsf

Focus Paper

The westward drift of the lithosphere: A tidal ratchet?

A. Carcaterra [a], C. Doglioni [b,c,*]

[a] Dipartimento di Ingegneria Meccanica e Aerospaziale, Sapienza University, Rome, Italy
[b] Istituto Nazionale di Geofisica e Vulcanologia, Rome, Italy
[c] Dipartimento di Scienze della Terra, Sapienza University, Rome, Italy

ARTICLE INFO

Article history:
Received 4 August 2017
Received in revised form
28 October 2017
Accepted 15 November 2017
Available online 6 December 2017
Handling Editor: M. Santosh

Keywords:
Westward drift of the lithosphere
Tectonic equator
Low-velocity layer
Asthenosphere viscosity
Non-linear rheology
Tidal ratchet

ABSTRACT

Is the westerly rotation of the lithosphere an ephemeral accidental recent phenomenon or is it a stable process of Earth's geodynamics? The reason why the tidal drag has been questioned as the mechanism determining the lithospheric shift relative to the underlying mantle is the apparent too high viscosity of the asthenosphere. However, plate boundaries asymmetries are a robust indication of the 'westerly' decoupling of the entire Earth's outer lithospheric shell and new studies support lower viscosities in the low-velocity layer (LVZ) atop the asthenosphere. Since the solid Earth tide oscillation is longer in one side relative to the other due to the contemporaneous Moon's revolution, we demonstrate that a non-linear rheological behavior is expected in the lithosphere mantle interplay. This may provide a sort of ratchet favoring lowering of the LVZ viscosity under shear, allowing decoupling in the LVZ and triggering the westerly motion of the lithosphere relative to the mantle.

1. Introduction

The lithosphere is broken in a number of plates (Bird, 2003) that move along a coherent mainstream, best defined by a sort of tectonic equator (Doglioni, 1993; Crespi et al., 2007). Moreover, the lithosphere has a "westerly" rotation relative to the underlying mantle (Le Pichon, 1968; Doglioni, 1993; Gripp and Gordon, 2002); however, its origin is still debated (Bostrom, 1971; Moore, 1973; Jordan, 1974; Ranalli, 2000; Scoppola et al., 2006; Riguzzi et al., 2010). As a function of the reference model, the rotation has been estimated either as a slow accidental residual (0.1°–0.2°/Ma) due to the faster "westerly"-directed motion of the Pacific plate (e.g., Ricard et al., 1991; Torsvik et al., 2010), or a much faster rotation (>1.1°–1.2°/Ma) affecting the entire external lithospheric shell, although segmented in plates having different velocities (Crespi et al., 2007; Cuffaro and Doglioni, 2007, 2017). Regardless of the rate, Pacific hotspots tracks like Hawaii demonstrate that the lithosphere shifts relative to the source of the hotspot, being the decoupling inferred within the low-velocity zone (LVZ), atop the asthenosphere (Fig. 1), which is in average between 100 and 200 km depth or even thinner (Rychert et al., 2005; Panza et al., 2010; Schmerr, 2012). Anderson (2011) and Rychert et al. (2013) have demonstrated that the last residence of the magma chamber beneath Hawaii is located at the top of the asthenosphere, within the LVZ, the inferred decoupling. Moreover, whatever are the origins of the hotspots and the rate of the net rotation (Doglioni et al., 2005), plate boundaries such as subduction and rift zones are asymmetric, supporting a global rotation of the lithosphere with respect to the mantle (e.g., Doglioni et al., 2007, 2015; Doglioni and Panza, 2015; Ficini et al., 2017), which is more consistent with the faster kinematic models and the global asymmetries along plate boundaries moving along the tectonic equator (Fig. 2). Moreover, the computation of the lithospheric volumes recycled in the mantle by subduction zones is about three times larger (about 230 km^3) along W-directed subduction zones with respect to the opposite E- or NE-directed slabs (about 70 km^3) as computed by Doglioni and Anderson (2015). This implies an 'easterly' directed mantle flow to compensate the volume unbalance. The tectonic equator represents the mainstream of plate motions and it is inclined 28°–30° relative to the geographic equator. This angle can be

* Corresponding author.
E-mail address: carlo.doglioni@uniroma1.it (C. Doglioni).
Peer-review under responsibility of China University of Geosciences (Beijing).

https://doi.org/10.1016/j.gsf.2017.11.009

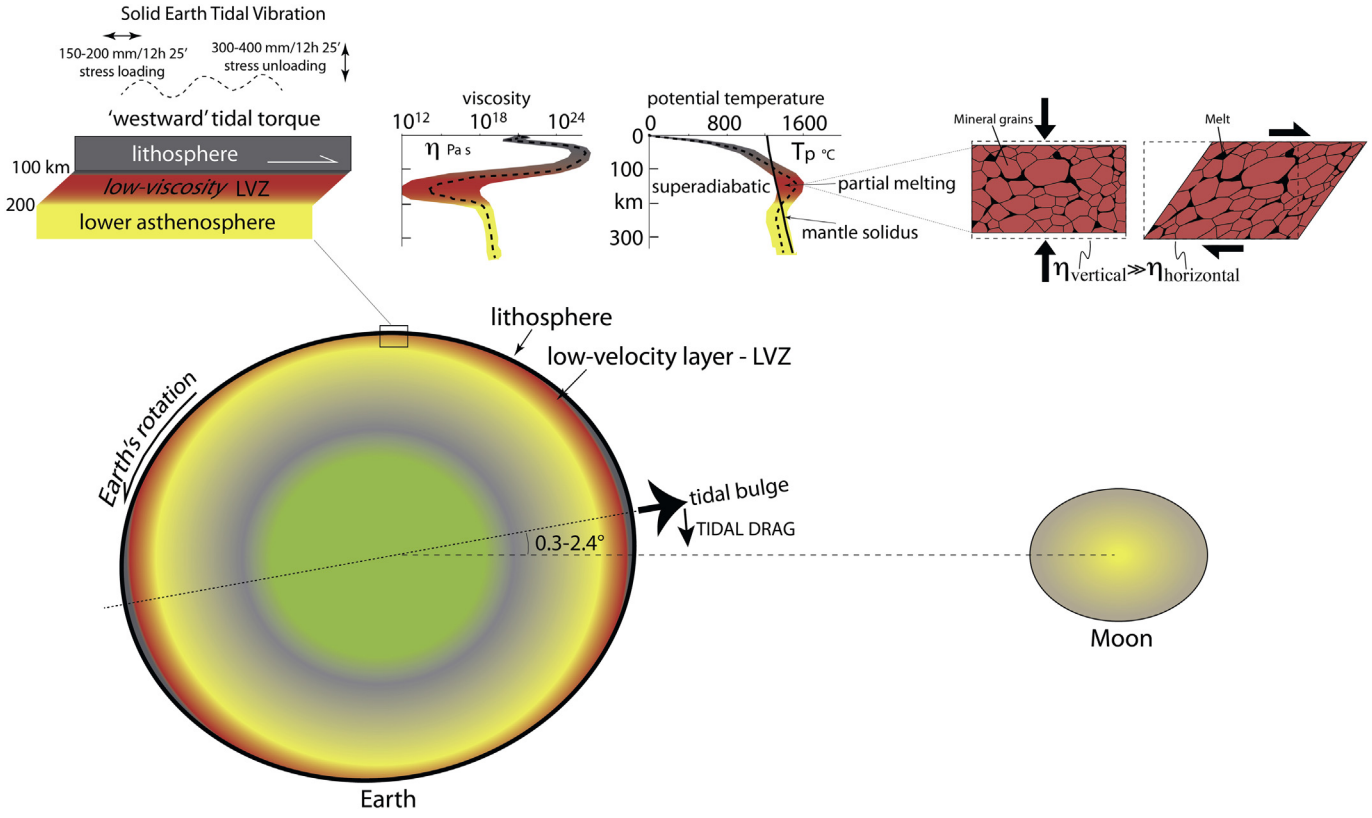

Figure 1. Simplified section of the Earth viewed from above the North Pole. The Earth is not perfectly elastic and it reacts with a few minutes delay to the Moon gravitation. Therefore the tidal bulge, exaggerated in the figure, is slightly misaligned relative to the Earth-Moon gravitational line. This generates a permanent torque toward the "west", opposite to the Earth's rotation, responsible for the tidal drag and the secular deceleration of the Earth's spin and the Moon's receding. The torque may also activate the "westward" drift of the lithosphere, relative to the underlying mantle, which is allowed by the presence of the low-velocity layer (LVZ). This layer has low viscosity due to the presence of partial melting. The effective viscosity in a granular layer with intervening melt in the pores is much smaller when measured for a shear parallel to the bedding (e.g. induced by horizontal plate motion) with respect to a vertical load (e.g., induced by ice formation or melting). The viscosity under shear is also assumed at least two orders of magnitude lower with respect to the vertical loading that is the usual way it is computed. The tidal torque occurs contemporaneously to the semidiurnal and diurnal tidal oscillations. This mechanical setting enhances a non-linear rheology of the mantle.

explained by the Earth's precession and the Maxwell time of the lithosphere. In fact the ratio between viscosity and rigidity is about 10^{12} s, i.e., the tectonic equator is the bisector of the angle generated by the oscillating Earth's axis that lasts 20,000–26,000 years (Doglioni and Panza, 2015; Cuffaro and Doglioni, 2017). The tectonic equator best represents also the net rotation or the westward drift of the lithosphere; moving toward the poles of the tectonic equator, plate velocities and seismicity at plate boundaries decrease, as well as ocean spreading rates and size of the orogens rates (Cuffaro and Doglioni, 2017). In their rotation along the mainstream, plates may also have a second sub-rotation that may apparently complicate or hinder the main flow (Cuffaro et al., 2008). It is important to note that the angle between the tectonic and the geographic equators is close to the sum of the inclination of the Earth's axis relative to the ecliptic plane (23°), plus the angle of the Moon's revolution around the Earth (5°).

The key question is: what causes the net rotation? Is it simply due to the fast motion of the Pacific plate toward the west-northwest due to the slab pull, or is it related to astronomical mechanisms such as the Earth's rotation and the consequent body tides generated on the solid Earth by the Moon and the Sun? An astronomical tuning of plate tectonics is suggested by seismicity decreasing toward polar areas (Riguzzi et al., 2010).

The slab pull is often invoked to explain the net rotation of the lithosphere (Ricard et al., 1991). However, the slab pull model is based on far too high values of negative buoyancy (e.g., 40–100 kg/m^3) with respect to the real Earth, where only the middle lithosphere can be inferred heavier than the underlying mantle of about 30–40 kg/m^3 maximum, but only in lenses within the lithospheric mantle (Afonso et al., 2008). Therefore, in average, the lithosphere ab-initio should have a bulk density in average lower than the underlying mantle. Subduction contributes to weigh the slab due to phase changes (van Keken et al., 2011). However, no relation among slab dip and age and temperature of the downgoing lithosphere can be observed (Cruciani et al., 2005). A long list of counterarguments on the slab pull efficiency is in Doglioni and Panza (2015). On the other hand, the tidal drag computed by Bostrom (1971) is energetically feasible for driving plate tectonics (e.g., Riguzzi et al., 2010). The main reason for discarding tidal drag as an effective mechanism to drift the lithosphere to the west has been so far the viscosity of the asthenosphere (Jordan, 1974; Ranalli, 2000). Values inferred from different techniques report variations from ultra-low viscosity (10^{12} Pa s, Jin et al., 1994) to much higher values (10^{19} Pa s, e.g., Cathles, 1975). Pollitz et al. (1998) and Hu et al. (2016) suggested values of 5×10^{17} Pa s. However, present techniques (e.g., glacial isostatic adjustment) are below the

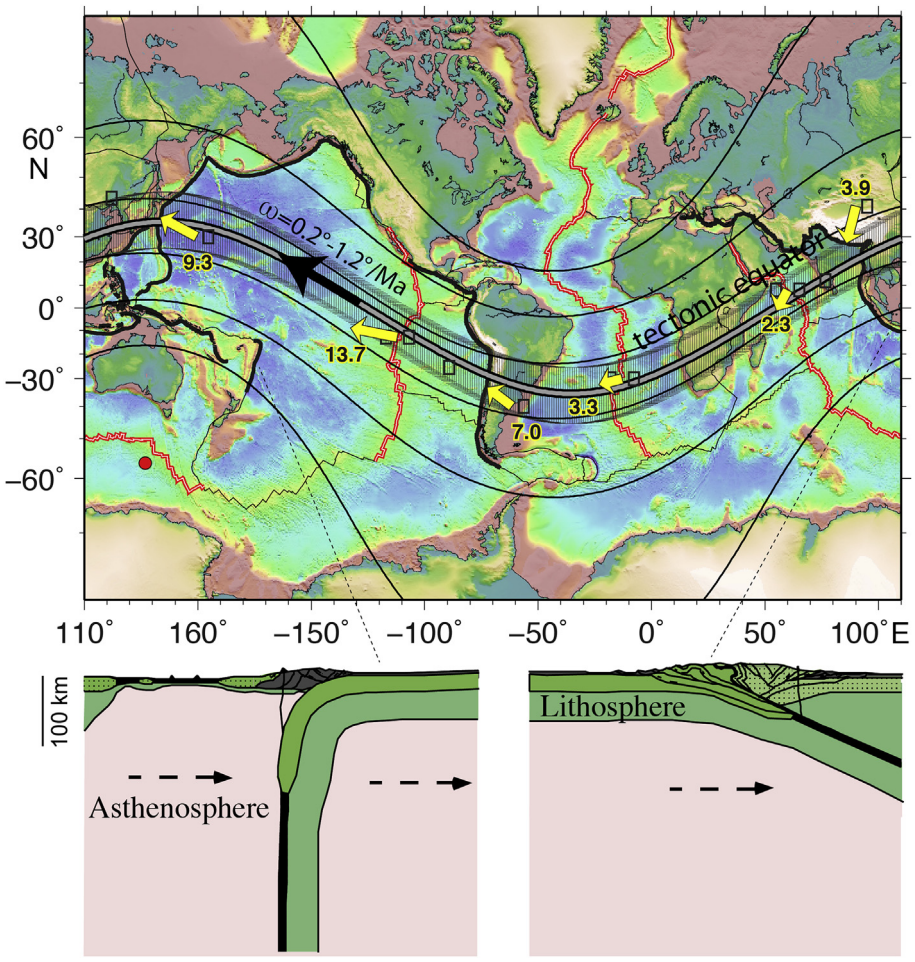

Figure 2. Mainstream of plate motions and trend of the tectonic equator that makes an angle of about 30° relative to the geographic equator. Yellow arrows indicate the relative velocity at major plate boundaries. The net rotation or westward drift of the lithosphere have been computed between 0.2°/Ma and 1.2°/Ma (thick black arrow) as a function of the hotspot reference frame. The red dot indicates the pole of rotation of the lithospheric rotation. The westward drift of the lithosphere implies that the underlying mantle is flowing 'easterly' relative to the lithosphere. Notice that all plate boundaries shift 'westerly' along the undulated flow relative to the mantle. Lower panel shows the main asymmetries at subduction zones consistent with the westward drift of the lithosphere (after Cuffaro and Doglioni, 2017).

detection threshold capability to resolve such a thin layer due to the channel flow model of Cathles (1975). Therefore, a thin low-viscosity layer at the top of the asthenosphere cannot be detected with present techniques and seismological resolution (Scoppola et al., 2006) and the values presented in the literature represent the bulk viscosity of the whole upper mantle or possibly the asthenosphere (Fig. 3), ignoring the LVZ that may actually represent the basal decoupling of the lithosphere. Higher resolution of viscosity in the LVZ may probably be reached by electromagnetic studies, showing higher conductivity at the lithosphere base of the Cocos plate (Naif et al., 2013). Here pargasite breakdown (Green et al., 2010) may explain the higher water content of the upper asthenosphere, generating a drastic decrease in viscosity and facilitating melting, a factor which also effectively lowers the LVZ viscosity (Kohlstedt and Hansen, 2015 and references therein). Moreover, a viscosity contrast of 8–10 orders of magnitude between the lithosphere and the asthenosphere can trigger decoupling between the two layers regardless their absolute value (Doglioni et al., 2011).

Another issue frequently ignored in viscosity computation is that the LVZ is more viscous under vertical loading or unloading with respect to horizontal shear. Intergranular partial melting may lower the viscosity up to three orders of magnitude (Fig. 1) as suggested by Scoppola et al. (2006). Similar results have been described by Hansen et al. (2012).

In this paper we present a new analytical model able to explain that even with a high bulk viscosity of the upper mantle, a relatively thin layer with reasonable lower viscosity can allow decoupling between lithosphere and asthenosphere driven by the tidal drag.

2. Model setup

Our model illustrates how the gravity force exerted by the Moon, in its relative motion with respect to the Earth, can potentially generate a circumferential drift of a tectonic plate (Fig. 4). A main result is that the tidal forces, besides the macroscopic well known oscillatory motions, can originate an unexpected one-way drift along directions tangent to the Earth surface. The model claims for a tidal ratchet effect borne from a nonlinear phenomenon that breaks the symmetry of the tidal force (Fig. 5). This phenomenon has analogy with phenomena observed in totally different fields, where the evolution of systems under unbiased external potentials have been observed, on average, directed one-

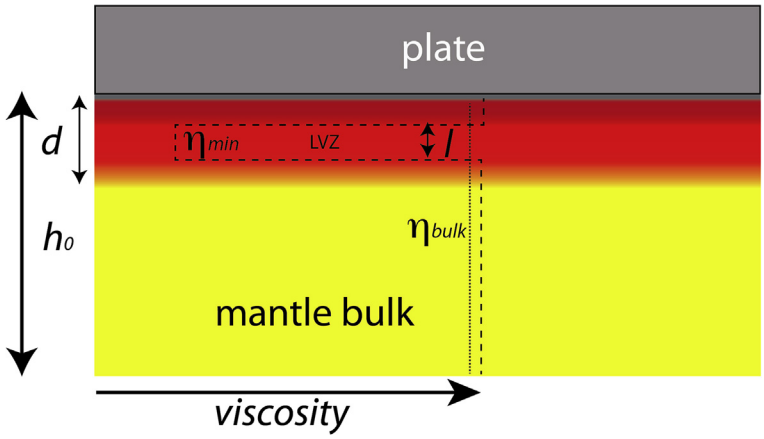

Figure 3. The occurrence of a few tens of km thick ultra low viscosity layer such as the low-velocity zone (LVZ) is invisible in the bulk viscosity of the upper mantle when computed with glacial isostatic rebound (Scoppola et al., 2006). Dashed line, simplified viscosity profile.

way (Leoncini et al., 2009). Examples come from plasma physics, through the transport effect born on charged electric particles in an oscillating electromagnetic field, or from Brownian motion immersed in an oscillating spatial periodic potential, or even from biological motors (Reimann, 2002).

We point out that the towing gravitational effect is caused by the tidal force distribution, as a dynamic process, since horizontal tidal force is seen at the Earth surface as a traveling wave load. This invests material points on the surface, producing their back and forth small motions, that are not perfectly symmetric. The small asymmetry produces a net drift motion of any material point interacting with the gravitational wave force, in the direction following the Moon's rotation. Drift is shown to be second order with respect to usual tidal oscillations.

This toy-model is conceived as a simplified analysis of more complex phenomena taking place during the gravitational mutual Earth-Moon interaction. Nevertheless, the proposed model provides a physical self-consistent mechanism to interpret the tectonic displacement as a nonlinear effect arising in the interplay between the gravitational force and the vertical distribution of viscous-elastic properties of the mantle.

More precisely, our analysis assumes moving point masses, equipped with rheological models controlled by a rather general transfer function (physically including elastic and viscous stress)

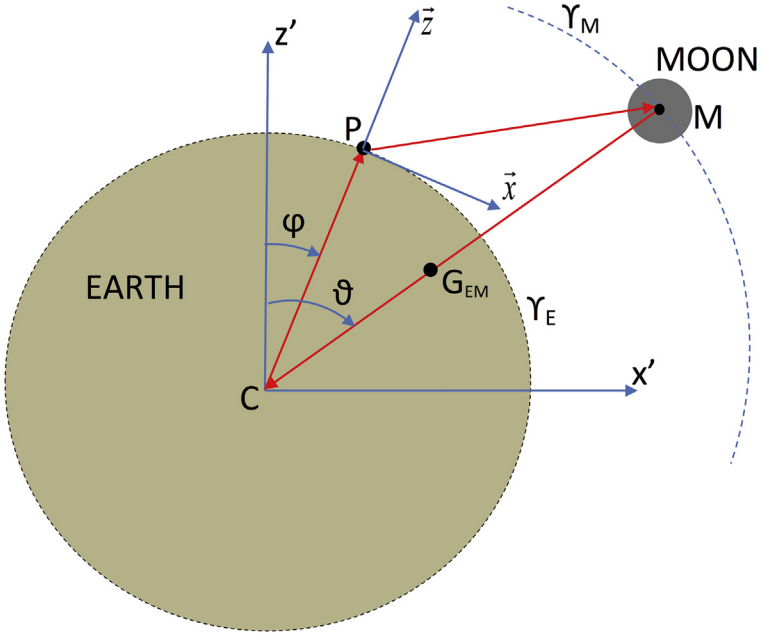

Figure 4. Sketch of the mechanical model of the Moon-plate interaction. M, Moon; P, plate; C, Earth center; G_{EM}, center of Earth-Moon mass. See text for explanation.

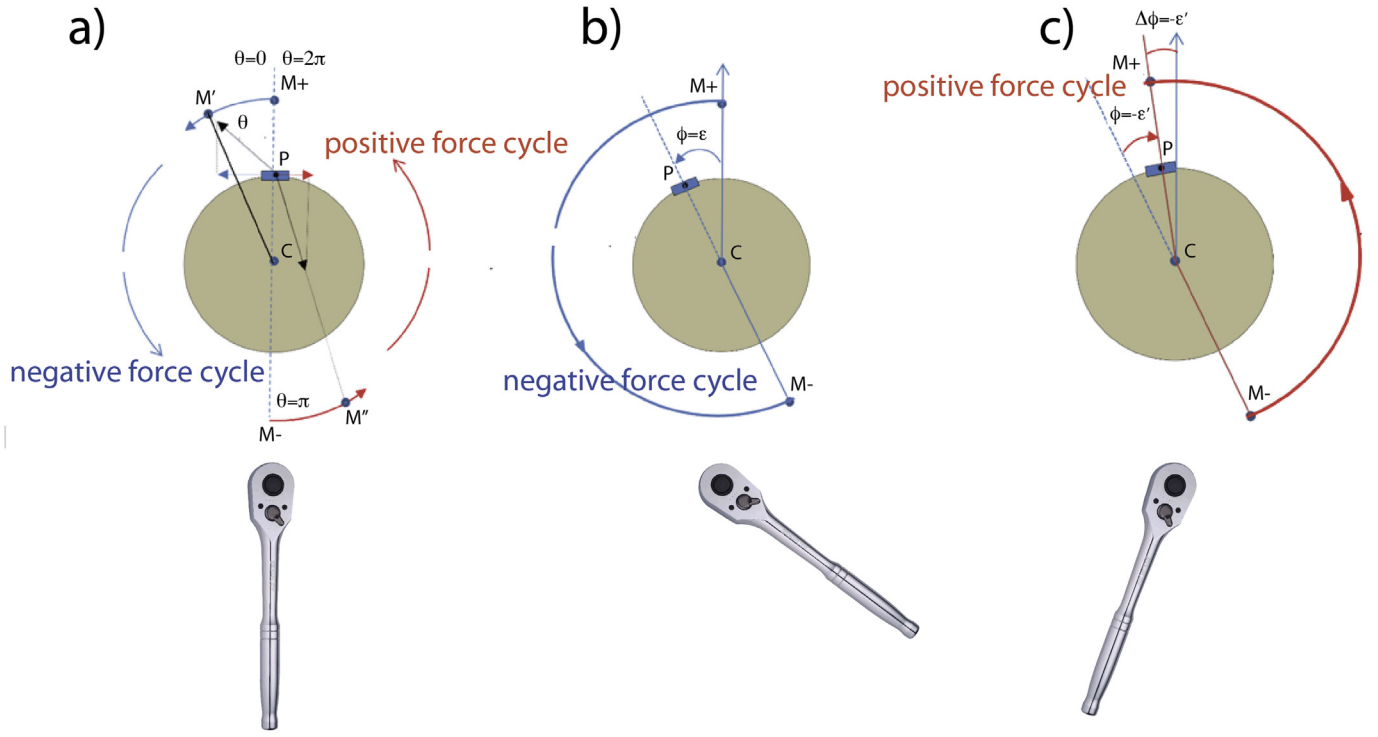

Figure 5. Asymmetric length of the body tide along the Earth's circumference due to the change in position of the Moon during the day. The body tide has a vertical and a horizontal component. The longer action of the horizontal component should determine a isoriented westerly directed torque, besides the torque exerted by the Earth's bulge misalignment, as the action of a ratchet. M, Moon; P, plate; C, Earth's center. See text for explanation.

and able to account for Newtonian, Maxwell, Voigt, Zener, Burgers and other generalized rheological models. In all these cases we see a daily tidal oscillation onto which a drift uniform motion of the tectonic plate is superimposed.

The Moon also is lumped into a point mass rotating over a circular orbit at a constant angular speed (with respect to the Earth), with its center collapsed into the Earth's one. Moreover, only the circumferential (tangent) motion of the mass is considered, neglecting any possible radial displacement both of the plate as well as of the inner mantle (Fig. 4). All these hypotheses can be even relaxed complicating the model, introducing an elliptic orbit (together with a variable Moon orbital speed) and a tidal radial motion; moreover, also the point mass associated to the surface plate can be expanded considering an elastic body of finite length over the circumference. However, all these effects are unnecessary to explain the plate drift, and have a weak qualitative influence in the present investigation, not inhibiting the outlined mechanism of drift generation.

The drift mechanism does not operate if the lithosphere is considered a perfect rigid body. In fact, the model needs the material particles on the Earth surface have some individual degree of mobility to be responsive to the traveling gravitational load. Therefore, detailed properties of the combined tidal oscillation and tidal drift can depend on the details of the rheology of the viscous-elastic lithosphere, not investigated here. Nevertheless, if the lithosphere has some degree of deformability, the described effect constantly appears. Final quantitative remarks about coupled plates systems are reported at the end of the paper.

One major result is that the tidal gravitation force lasts slightly longer when the plate on the Earth surface is rotating in the sense of the Moon's revolution, because of a non-linear behavior, and a tiny permanent westward displacement once a day appears. Under some assumptions, we determine an analytical expression for the drift velocity of the plate due to this mechanism. A physical interpretation of the mathematical model described above is given by means of simple mechanical considerations.

3. Method

In Fig. 4, the Earth's reference systems is $R_{Cx'y'}$. The angles that at the time t CM and CP form with x′, are $\vartheta(t)$ and $\varphi(t)$, respectively. The Moon M, with mass m, is rotating over the circumference γ_M (of radius R) at a constant angular speed ω_M with respect to the Earth. The period of the Moon rotation is T_M. The motion of the plate P, with mass m_p, in the reference frame $R_{Cx'y'}$ is described by φ, with the plate running over the circumference γ_E of radius r and center C. Finally, $\vec{x}$, $\vec{z}$ are the local tangent and normal unit vectors along γ_E. G_{em} is the gravity center of the Moon-Earth pair, at radial distance $R_G \approx (3/4)r$ from the Earth's center C, and along CM. The Moon-Earth system rotates about G_{em}, generating on the point masses on the Earth an inertial force field $\overrightarrow{f_{in}}$ usually estimated equal to the center C centrifugal force. The gravitational force $\overrightarrow{f_g}$ the Moon exerts on the generic point mass m_P at P_z, and $\overrightarrow{f_{in}}$ at the same point P_z, have form:

$$\overrightarrow{f_g} = G\frac{m\,m_P}{\left|\overrightarrow{P_zM}\right|^3}\overrightarrow{P_zM},\quad \overrightarrow{f_{in}} = G\frac{m\,m_P}{R^2R_G}\overrightarrow{G_{em}C}$$

$$\overrightarrow{P_zM} = \begin{Bmatrix} R\sin\vartheta - z\sin\varphi \\ R\cos\vartheta - z\cos\varphi \end{Bmatrix},\ \overrightarrow{G_{em}C} = \begin{Bmatrix} -R_G\sin\vartheta \\ -R_G\cos\vartheta \end{Bmatrix} \quad (1)$$

The vectors components refer to the Earth's reference system, and G is the gravitation constant. Tidal force is borne as a

superposition of the Moon's gravity force at each point on the Earth, and the inertial force, i.e. it is $\overrightarrow{f_g} + \overrightarrow{f_{in}}$, at any point P_z on the Earth, and has component f_x along z and at any angle φ

$$f_x(\varphi-\vartheta,z) = \left(\overrightarrow{f_g}+\overrightarrow{f_{in}}\right)\cdot\vec{x} = f_0 F(\vartheta-\varphi,z)$$
$$\vec{x} = \left\{\begin{array}{c}\cos\varphi\\ -\sin\varphi\end{array}\right\},\quad f_0 = G\frac{m\,m_P}{R^2}$$
$$\chi(\vartheta-\varphi,z) = \left[1+\delta^2-2\delta\cos(\vartheta-\varphi)\right]^{3/2}$$
$$\delta = \frac{z}{R},\quad F(\vartheta-\varphi,z) = \left[\frac{1}{\chi(\vartheta-\varphi,z)}-1\right]\sin(\vartheta-\varphi)$$
$$\vartheta = \omega_M t \qquad (2)$$

In case the point mass P_z identifies the plate P on the Earth's surface, i.e. $z = r$, its equation of motion along γ_E is:

$$m_P\, r\,\ddot{\varphi}(t) + A\,\tau_{xz}(t,r) = f_x(\vartheta-\varphi,r) \qquad (3)$$

where A is the plate surface, $\tau_{xz}(t,r)$ the shear stress at $z = r$.

A good approximation of the tidal force (1), used in the following and usually accepted in the scientific literature (Elmore and Heald, 1969), comes from the small parameter $\delta = z/R < r/R \ll 1$, that makes it possible the first order Taylor series for F in terms of δ:

$$F(\vartheta-\varphi,\delta) \approx \frac{3}{2}\,\delta\,\sin(2\omega_M t - 2\varphi) \qquad (4)$$

This expression represents a wave load traveling over the Earth surface at speed $c_{wg} = \omega_M\, r$.

While a strict analysis of the solution to Eq. (3) with Eq. (4) is examined later, the underlying physical mechanism leading to the plate drift motion excited by the wave load (Eq. (4)), can be outlined on the basis of more intuitive mechanical considerations.

As first, we can study a single force cycle the Moon exerts on the plate during a single rotation about the Earth, over a half period $T_M/2$ being the entire phenomenon just a repeated sequence of similar cycles with alternate signs.

At any point P, $\overrightarrow{f_g} + \overrightarrow{f_{in}}$ exhibits normal and tangent components, respectively. The last is of interest in the plate drift phenomenon studied here. Space distribution of both forces along the Earth's circumference (as it appears from Eqs. (2) and (4) for the tangent component) follows approximately sine and cosine functions, respectively, that wrap the Earth completing two periods along the circumference (or twice a day). The main known effects of tidal force are the almost ellipsoidal shape deformation of the Earth and the ocean tides. We show here an additional important property of the tangent tidal component. In fact, any tidal oscillation on the Earth surface, is shown to have as side effect, an associated very slow, one-way, drift motion, following the Moon's rotation, that can form the basis for the tectonic plates motion.

The polar diagram of the tangent force distribution provided by Eq. (4) is depicted in Fig. 6. It consists of four lobes. Two produce a positive tangent component, represented by red curves, the other two, represented by blue curves, produce a negative force on the plate P. Since this force distribution is perceived, by an observer on the Earth, as a traveling wave force, the diagram rotates following the Moon. Three successive configurations along the Moon's rotation are sketched in Fig. 6a–c. We start with the Moon, the plate and the Earth centers M, P and C, respectively, along the same line (Fig. 6a). In the absence of any displacement of the plate P, the Moon, completing a single relative rotation about the Earth, exerts on the plate a tangent force f_x having zero average. In fact, each lobe covers 90° and positive and negative forces simply alternate along angles of equal extent (namely 90° each), so that at each fixed point over the Earth surface the average force is zero.

The zero towing effect of this configuration, would amount to the symmetry of the problem when neglecting the small plate motion, that is indeed certainly present because of the applied traveling force. In fact, in the first quarter force cycle, corresponding roughly to 90° of Moon clockwise rotation, the plate is subjected to the positive half-wavelength tidal force, and starts along the positive angular clockwise direction, following the Moon rotation. The plate P describes during this interval a very small angle $\Delta\varphi_{\text{Positive}}$ under the tidal force and the viscous resistance of the mantle (in Fig. 6b it is magnified to make the effect more visible). Due to this small drift motion of the plate, the positive force cycle ends with a delay with respect to the expected 90° of Moon clockwise rotation, and namely after an angle $90° + \Delta\varphi_{\text{Positive}}$ of Moon rotation, since the plate is moving in the same direction of the tidal traveling force (see Fig. 6b). Then the plate exits its positive force cycle, and enters the second half-wavelength of negative tidal force (see Fig. 6c). In this second quarter force cycle, the plate moves anticlockwise, opposite to the Moon rotation. The duration of this second phase is for this reason shorter than the first, and covers an angle of Moon rotation equal to $90° - \Delta\varphi_{\text{Negative}}$. The third and the forth force cycles repeat an identical scheme. This phenomenon amounts to a net drift rotation $\Delta\varphi_{\text{Drift}} = 2(\Delta\varphi_{\text{Positive}} - \Delta\varphi_{\text{Negative}})$ of the plate for any complete rotation of the Moon about the Earth.

With this brief analysis, we conclude that the force tidal tangent distribution produces an important side effect associated to the tidal oscillation $\Delta\varphi_{\text{Tidal}} = 1/2(\Delta\varphi_{\text{Negative}} + \Delta\varphi_{\text{Positive}})$: it is a net drift rotation of the plate measured by an angular speed $\omega_{\text{Drift}} = \Delta\varphi_{\text{Drift}}/T_M/2 = 2/T_M(\Delta\varphi_{\text{Positive}} - \Delta\varphi_{\text{Negative}})$. The typical qualitative trend of the angle of rotation of the plate follows as plotted in Fig. 6d.

The drift effect is borne by the wave force symmetry breaking due to the small plate displacement under the action of the traveling wave force caused by the Moon's gravitation. Mathematical counterpart for this effect is in Eq. (3), where the force $f_x(\vartheta-\varphi,r)$ depends nonlinearly on the plate rotation. This physical effect is similar to the ponderomotive force met when an electron is traveling into an electromagnetic wave. Note that the plate is assimilated here to a single material point sliding over the Earth surface. Reality is more complex, but this drifting effect is definitely driving the motion of all the material points of the crust, the mantle and deeper layers, provided that they have a degree of relative mobility, i.e. they belong to a deformable material body.

One important geodynamic condition to support this model is that of a viscous drag that allows for a sufficient degree of mobility of the point plate, such that the difference between the fluctuations $\Delta\varphi_{\text{Positive}} - \Delta\varphi_{\text{Negative}}$ is large enough to be in agreement with the annual drift displacement observed for the tectonic plates, or to be a component of the driving plate process. Global estimates of Earth's viscosity, meaning reference single average values of the mantle viscosity, are not suitable since a key role is played by the vertical distribution of viscosity, by its gradients and by the details of the rheological model of the mantle.

Therefore, a second important element arising from the model is the comparison between the effective viscosity η_{eff} and the average viscosity $\overline{\eta}$ of the mantle. It appears that the two values η_{eff} and $\overline{\eta}$, can be considerably different, showing in this way that even for a mantle bulk with a large average viscosity, the drag experienced on its surface from the plate, can be equivalent to an effective viscosity that is several order of magnitude less than the average viscosity of the profile.

This remark suggests a certain carefulness in the formulation of arguments against the chance of the tectonic plate motion driven

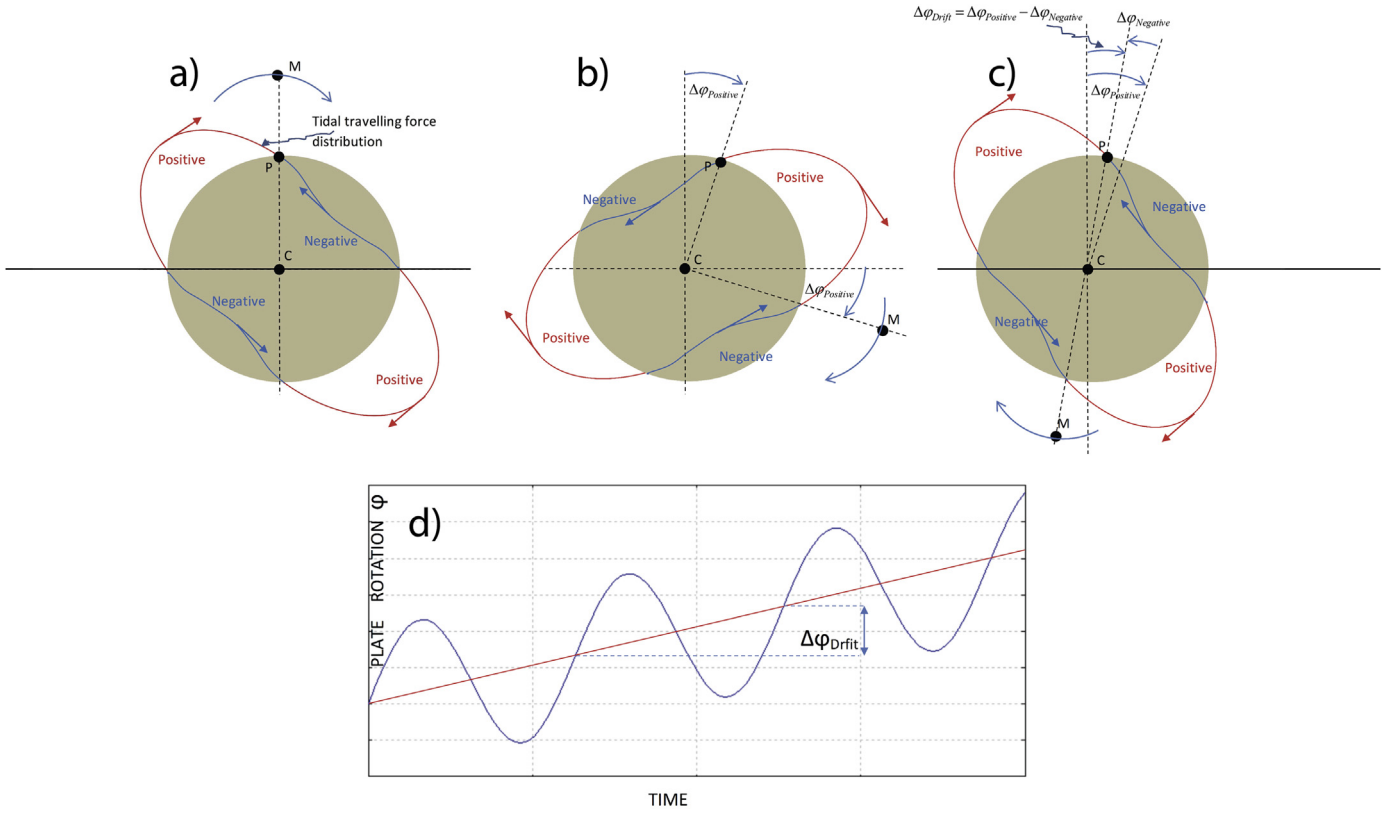

Figure 6. Mechanical model for the westerly directed lithospheric drift. Panel (a): Moon (M), the plate (P) and the Earth (C) centers are initially aligned. In the absence of any displacement of the plate, the Moon, completing a single relative revolution about the Earth, exerts on the plate a tangent force having zero average, implying at the end of the cycle, the cumulative net plate response amounts to zero. The zero towing effect of this configuration, would amount to the symmetry of the problem when neglecting the small plate motion that is indeed certainly present because of the applied traveling force. In fact, in the first quarter force cycle, corresponding roughly to 90° of Moon clockwise rotation, the plate is subjected to the positive half-wavelength tidal force, and starts along the positive angular clockwise direction, following the Moon rotation. The plate P describes during this interval a very small angle under the tidal force and the viscous resistance of the mantle (in Panel b it is magnified to make the effect more visible). Due to this small drift motion of the plate, the positive force cycle ends with a delay with respect to the expected 90° of Moon clockwise rotation, and namely after an angle 90°+ of Moon rotation, since the plate is moving in the same direction of the tidal traveling force (see Panel b). Then the plate exits its positive force cycle, and enters the second half-wavelength of negative tidal force (see Panel c). In this second quarter force cycle, the plate moves anticlockwise opposite to the Moon rotation. The duration of this second phase is shorter than the first, and covers an angle of Moon rotation equal to 90°−. The third and the forth force cycles repeat an identical scheme. This phenomenon amounts to a net drift rotation of the plate for any complete revolutionn of the Moon about the Earth. Lower panel (d): typical trend of the angle of rotation of the plate: oscillatory motion is superimposed to a linear trend related to the plate drift motion. See text for explanation.

by the Moon, based on oversimplified models that refer to a generic single value of the viscosity considered as “too high” (Jordan, 1974).

To make an exemplification related to the distinction between average and effective viscosity, consider a profile of viscosity as in Fig. 3.

This is piecewise constant, corresponding to an idealized case of a bulk of total depth h_0 with a constant viscosity η_{bulk} into which a low viscosity channel exists, a layer of thickness l and depth d in the vertical distribution, and with a lower viscosity $\eta_{\min}$. For a small thickness l with respect to h_0, we obtain (by elemental physics) the approximations $\overline{\eta} \approx \eta_{\text{bulk}}$ and $\eta_{eff} \approx (h_0/l)\eta_{\min}$. This comparison shows that the effective viscosity, the one perceived by the plate as a drag effect, is essentially close to the minimum values along the vertical viscosity profile, and inversely proportional to the thickness of the low velocity layer. The presence in recent studies of a channel with a thin layer of low viscosity makes the effective viscosity very low, even if the bulk of the mantle has, on average, much larger values (Scoppola et al., 2006). In this case the minimum viscosity is several order of magnitude less than the average and even the existence of a thin low viscosity layer (for example about 20 km), characterized by a ratio $h_0/l \approx 10 \div 10^2$ can produce an effective viscosity of about 9–11 orders of magnitude less than expected form the bulk average viscosity.

An additional element modifying the drag experienced by the plate is that the viscosity, for a large class of rheological behaviors, appears to be frequency dependent (in general decreasing for an increasing frequency).

Finally, the gravitational traveling load acts not only on the Earth surface, i.e. directly on the plate, but also on the deeper layers of the Earth, producing a further reduction of the perceived drag from the plate and the effective viscosity of the materials underlying the plate.

The previous arguments outline a nonlinear mechanism that induces a plate drift effect besides tidal oscillations. This process, combined with the chance of a reduced drag experienced by the plate due to an effective viscosity much smaller than the average viscosity of the mantle and the pulling effect also on deeper layers, permits a plate motion sufficient to incept this nonlinear mechanism. Since recent studies (Scoppola et al., 2006) support the idea of a low viscosity channel in the upper asthenosphere, corresponding to the low velocity layer, even if of small thickness, we conclude that the mechanism of plate motion driven by the Moon gravity force is feasible and leads to plate speed compatible with the experimental ones.

The analysis ahead provides mathematical basis to solution to Eq. (3) keeping the outlined mechanisms.

To complete Eq. (3), the expression of the interaction force $A\tau_{xz}(t,r)$ between the plate and the mantle must be determined.

In the present analysis, the rheological model is by a τ-γ relationship (Mainardi and Spada, 2011, and references therein)

$$\sum_{k=0}^{N}\alpha_k\frac{d^k\tau_{xz}}{dt^k}=\sum_{h=1}^{M}\beta_k\frac{d^k\gamma_{xz}}{dt^k} \tag{5}$$

where $d\gamma_{xz}/dt$ is the strain rate. Equation (5) includes rheological models as Newtonian, Maxwell, Zener, Burgers and other generalizations, such as frequency dependent viscosity. The constitutive relationship along the depth z, in the Laplace domain, reads $\widehat{\tau}_{xz}(s,z)=H(s,z)\,\widehat{\gamma}_{xz}(s,z)$, $H(s,z)=N(s,z)/D(s,z)=\sum_{k=1}^{M}\beta_k(z)s^k/\sum_{k=0}^{N}\alpha_k(z)s^k$ and the hat denotes Laplace transform with respect to time, $\alpha_k(z)$, $\beta_k(z)$ in general complex quantities identifying rheological properties at different depth.

The differential equation for the mantle shear stress distribution along the radial direction z is assumed (neglecting inertial forces and with $\widehat{\gamma}_{xz}=(1/2s)(\partial\widehat{v}_x/\partial z)$) as:

$$\frac{\partial\,\tau_{xz}(t,z)}{\partial\,z}+\frac{\rho}{m_p}f_x(t,\,z)=0 \tag{6}$$

where now it would be $f_x(t,z)\approx(3/2)(z/R)f_0\,\sin[2\omega_M t-2\varphi(t,z)]$ introducing the rotation angle of the particles at any depth z. However, since the low viscosity layer is located at small depth compared to r, we approximate the z dependence in the pulling force as $f_x(t,z)\approx(3/2)(z/R)f_0\,\sin[2\omega_M t-2\varphi(t)]$.

Integrating twice, the shear velocity in the Laplace domain is approximated as:

$$\widehat{v}_x(s,z)=\alpha(s)\int_{z_0}^{z}\frac{2s\,dz'}{H(s,z')}-\frac{\rho}{m_p}\int_{z_0}^{z}\frac{2s}{H(s,z')}\int_{z_0}^{z'}\widehat{f}_x(z'',s)dz''dz'+\widehat{v}_x(s,z_0) \tag{7}$$

$\alpha(s)$ and $\widehat{v}_x(s,z_0)$ are suitable integration constants to be determined assigning appropriate boundary conditions at the surface $z=r$, and at the bottom $z=z_0$. Integration starts at z_0, and one bottom boundary condition can be imposed at the depth where the shear velocity $\widehat{v}_x(s,z_0)$ vanishes. This reasonably occurs where the vertical axis z meets a solid and rigid surface, the points of which are at rest with a null tangent velocity. This bottom surface can be identified with the inner solid core (at depth $z=z_0$), where we assume $\widehat{v}_x(s,z_0)=0$. The second boundary condition, at the Earth's surface ($z=r$), implies:

$$\alpha(s)=\frac{\widehat{v}_x(s,r)}{I(s)}+\frac{\rho}{m_p}\int_{z_0}^{r}\frac{2s}{I(s)H(s,z)}\int_{z_0}^{z}\widehat{f}_x\left(t,z'\right)dz'dz \tag{8}$$

$$I(s)=\int_{z_0}^{r}\frac{2s\,dz}{H(s,z)}$$

To simplify, the following analysis assumes $H(s,z)=\beta_1(z)s+\sum_{k=2}^{M}\beta_k s^k/\sum_{k=0}^{N}\alpha_k s^k$, where the dependence on z is affecting only the steady part of the viscosity related coefficient $\eta=\beta_1(z)$, since for it a strong variability along z is known from the scientific literature (Cadek and van den Berg, 1998, and references therein). More precisely, we know that a low viscosity channel exists at a depth of about 100–200 km under the lithosphere (Riguzzi et al., 2010), where the viscosity is lowered by more than 10 orders of magnitude, strongly affecting the dynamics of the plate on the Earth surface. Let us approximate the vertical viscosity along z, following the investigations of Scoppola et al. (2006) with a constant piecewise distribution

$$\begin{cases}\eta=\beta_{bulk}\ \text{ for }\ z\in[z_0,z_L],\,z\in[z_L+l,r]\\ \eta=\beta_{1min}\ \text{ for }\ z\in[z_L,z_L+l]\\ \beta_{1min}<<\beta_{bulk},\quad l<<z_L.\end{cases}$$

With these approximations, in the following we use the symbols $H=H(s)|_{\beta_1=\beta_{1\,\min}}$, $N=N(s)|_{\beta_1=\beta_{1\,\min}}$, $D=D(s)$, $J=3(1+z_L\,d/h\,r)$, $d=r-z_L$, and the plate equation of motion finally reads:

$$\left[m_p r\,D\,s^2+\frac{A}{2}\frac{r}{l}N\right]\widehat{\varphi}(s)=\frac{J}{3}f_0 D\,\widehat{F} \tag{9}$$

The expression for J shows the second term $z_L d/hr$ that accounts for the pulling gravitational effect on the deeper layers of the mantle (the first addend of J is that directly acting on the plate). Moreover, N and D are calculated at the low viscosity zone, showing that the dominant viscosity comes from that region. In general, this nonlinear equation, and its time domain differential counterpart as well, are not available for any analytical solution. However, a perturbation approach makes it possible to enlighten the separation of a plate drift slow motion phenomenon from the superimposed faster tidal oscillations.

Using the approximation Eq. (4), transforming back to time domain with $\tau=t/T_M$, and assuming a parallelepiped shape for the plate, i.e. using $m_p=A\rho h$, one obtains:

$$\Pi\sum_{k=0}^{N}\frac{\alpha_k}{T_M^k}\frac{d^{k+2}\varphi(\tau)}{d\tau^{k+2}}+\sum_{k=1}^{M}\frac{\beta_k/\beta_{1\min}}{T_M^{k-1}}\frac{d^k\varphi(\tau)}{d\tau^k}=\varepsilon\frac{Jl}{R}\sum_{k=0}^{N}\frac{\alpha_k}{T_M^k}\frac{d^k}{d\tau^k}\sin(4\pi\tau-2\varphi) \tag{10}$$

where $\varepsilon=f_0T_M/A\beta_{1\,\min}$, $\Pi=2\rho hl/\beta_{1\,\min}T_M$.

The physical key to determine φ from Eq. (10) in an analytical form relies on the chance to examine the plate motion when the plate rotation φ is small with respect to the Moon's rotation $\omega_M t$. This means we are interested in solutions for which $\left|\dot{\varphi}\right|<<\omega_M t$ or $\left|\dot{\varphi}\right|\omega_M<<1$, that is very close to what happens in reality. The dimensionless parameter $\varepsilon=f_0T_M/A\beta_{1\,\min}$ is of the order of magnitude of $\left|\dot{\varphi}\right|/\omega_M$. In fact, it expresses the ratio between the effect of the Moon's gravitation force f_0 on the plate, and the shear viscous resistance of the lithosphere with an order of magnitude $A\,\beta_{1\min}\dot{\varphi}$. The equilibrium of these forces produces $\dot{\varphi}\propto f_0/A\,\beta_{1\min}$ and $\dot{\varphi}/\omega_M\propto f_0\,T_M/A\,\beta_{1\min}=\varepsilon<<1$. This makes it possible to use a perturbation expansion $\varphi=\varphi_0+\varepsilon\varphi_1+\varepsilon^2\varphi_2$ for the plate motion, identifying two different amplitude scales for the force and tidal response as ε, ε^2.

Before illustrating the general solution to Eq. (10), let us consider a particular case, that shows the tidal ratchet in its simplest form. In fact, assuming a Newtonian rheological model, the equation simplifies as:

$$\frac{d\varphi}{d\tau}=a\,\sin(4\pi\tau-2\varphi),\quad a=\varepsilon\frac{J\,l}{R} \tag{11}$$

that still preserves the fundamental nature of the ratchet effect and where the parameter a is small (it contains ε). In fact, for Eq. (11), an analytical solution exists:

$$\varphi(\tau) = 2\pi\tau - tg^{-1}\left[\frac{\sqrt{4\pi^2 - a^2}\,tg\left[(\tau+\tau_0)\sqrt{4\pi^2 - a^2}\right] + a}{2\pi}\right] \tag{12}$$

where the constant τ_0 is to fit initial conditions for $\varphi(0)$. Mechanical interpretation of Eq. (12) is easier if we expand this solution in terms of the small parameter a:

$$\varphi(\tau) = -2\pi\tau_0 - \frac{a}{2\pi}\cos^2(2\pi(\tau+\tau_0)) + \frac{a^2}{4\pi}(\tau+\tau_0) + \frac{a^2}{32\pi^2}[4\sin(4\pi(\tau+\tau_0)) + \sin(8\pi(\tau+\tau_0))] \tag{13}$$

from which the ratchet effect $(a^2/4\pi)\tau$ comes out and amounts to a linear growth, second order with respect to the tidal oscillation $a/2\pi\cos^2(2\pi(\tau+\tau_0))$. A one-directional motion is borne because of the nonlinear nature of the process. From this, the ratchet angular speed $\omega_{\text{Ratchet}} = a^2/4\pi\,T_M$ follows a basic result of this paper. Since the second order term $(a^2/4\pi)\tau$ growing in time is dominant with respect to the oscillating term $a^2/32\pi^2[4\sin(4\pi(\tau+\tau_0)) + \sin(8\pi(\tau+\tau_0))]$, we have the approximate expression:

$$\varphi(\tau) \approx -2\pi\tau_0 - \frac{a}{4\pi}\cos(4\pi(\tau+\tau_0)) + \frac{a^2}{4\pi}\tau \tag{14}$$

Exact analytical solutions as (14) are not possible when the equation of motion has additional terms as for Eq. (10), but a perturbation approach with $\varphi = \varphi_0 + a\varphi_1 + a^2\varphi_2$ (or $\varphi = \varphi_0 + \varepsilon\varphi_1 + \varepsilon^2\varphi_2$) still produces the ratchet effect and it is applicable even in the more complex case of Eq. (10). To show how to proceed, let us illustrate for comparison the perturbation approach to Eq. (11). Substituting $\varphi = \varphi_0 + a\varphi_1 + a^2\varphi_2$ into Eq. (11) produces the perturbation cascade:

$$\begin{aligned}\frac{d\varphi_0}{d\tau} &= 0\\ \frac{d\varphi_1}{d\tau} &= \sin(4\pi\tau - 2\varphi_0)\\ \frac{d\varphi_2}{d\tau} &= -2\varphi_1\cos(4\pi\tau - 2\varphi_0)\end{aligned} \tag{15}$$

the solution of which is:

$$\varphi(\tau) = \psi_0 - \frac{a}{4\pi}\cos(4\pi\tau - 2\psi_0) + \frac{a^2}{4\pi}\tau + \frac{a^2}{32\pi^2}\sin(8\pi\tau - 4\psi_0) \tag{16}$$

where ψ_0 is the constant to fit the initial condition. Neglecting the second order oscillating term with respect to the linearly growing $(a^2/4\pi)\tau$, we obtain:

$$\varphi(\tau) \approx \psi_0 - \frac{a}{4\pi}\cos(4\pi\tau - 2\psi_0) + \frac{a^2}{4\pi}\tau \tag{17}$$

Comparison between Eqs. (17) and (14) shows they are identical, provided that integration constants are chosen as $\psi_0 = -2\pi\tau_0$. The same perturbation analysis is carried on for Eq. (10). After conceptually similar calculations for Eq. (10), the complete physically significant solution to the plate equation of motion is:

$$\varphi(\tau) = \varepsilon\varphi_1(\tau) + \varepsilon^2\varphi_2(\tau) = \varepsilon(Z_I\cos 4\pi\tau + Z_R\sin 4\pi\tau) - \varepsilon^2\frac{Jl}{R}Z_I\tau \tag{18}$$

$$Z = Z_I + jZ_R = \frac{J\,l}{R}\frac{\sum_{k=0}^{N}\frac{\alpha_k}{T_M^k}(4\pi j)^k}{\Pi\sum_{k=0}^{N}\frac{\alpha_k}{T_M^k}(4\pi j)^{k+2} + \sum_{k=1}^{M}\frac{\beta_k/\beta_{1\min}}{T_M^{k-1}}(4\pi j)^k} = -\frac{J\,l}{R}\frac{1}{(4\pi)^2\Pi - \frac{T_M}{\eta_{\min}}H(2\omega_M)} \tag{19}$$

The solution Eq. (18) includes the first order oscillatory terms only, the second order oscillatory ones, yet produced by the perturbation approach, are indeed neglected. The term $-\varepsilon^2(J\,l/R)Z_I\tau$, linearly increasing with time, demonstrates the drift motion as a second order quantity associated to the first order tidal oscillation. The amplitude of tidal oscillation $\Delta\varphi_{\text{Tidal}}$ and the drift angular speed ω_{Drift} are respectively:

$$\omega_{\text{Drift}} = -\varepsilon^2\frac{J\,l}{R}\frac{Z_I}{T_M}, \quad \Delta\varphi_{\text{Tidal}} = \varepsilon|Z| \tag{20}$$

that is a key result of this paper. The complex number Z contains the rheology model of the mantle, besides the minimum viscosity appearing in ε. The factor $J\,l/R$ contains the information on the depth and thickness of the low viscosity layer. Turning back to the initial mechanical explanation of the model, Eq. (20) determine the quantitative value for the drift angle as $\Delta\varphi_{\text{Drift}} = \Delta\varphi_{\text{Positive}} - \Delta\varphi_{\text{Negative}} = -\varepsilon^2(J\,l/R)\,Z_I$, and Eq. (18) supports the trend qualitatively depicted in Fig. 6.

Note that Eq. (20) can provide values of the drift angular speed largely depending on the choice of the rheological model. In other words, we can conclude that a tidal drift due to the Moon gravitation exists, and its quantitative effect remains with the Earth rheology.

However, from $\omega_{\text{Drift}} = -\varepsilon^2(J\,l/R)(Z_I/T_M)$, one can attempt to determine an inverse formula to estimate some rheological parameters assuming $\omega_{\text{Drift}} \approx 10^{-16}$ rad s^{-1} (Jordan, 1974, corresponding to a plate drift of about 2 cm/year), an average physical significant value for plate tectonics annual drift.

From the general Eq. (19), we can assume a particular model for Z in the form:

$$Z = -j\frac{J\,l}{4\pi\,R}\frac{\eta_{\min}}{\eta_{\min} + \sum_{k=2}^{M}\left(\frac{4\pi}{T_M}\right)^{k-1}p_{k-1}} \tag{21}$$

assuming β_k pure imaginary or real for even k, or odd k, respectively, i.e. $\beta_k = (-j)^{k-1}p_{k-1}$ with p_k real and $\alpha_0 = 1$, $\alpha_k = 0$, $k = 1, 2\ldots$. This choice has a simple physical interpretation. In fact, this implies $H = \sum_{k=1}^{M}\beta_k s^k = j\omega(\sum_{k=1}^{M}p_{k-1}\omega^{k-1}) = j\omega(\eta_{\min} + \sum_{k=2}^{M}p_{k-1}\omega^{k-1})$, meaning we introduce the frequency dependent viscosity $\eta(\omega) = \eta_{\min} + \sum_{k=2}^{M}p_{k-1}\omega^{k-1} = \eta_{\min} - \mu(\omega)$, as it happens frequently for a large class of rheological behaviors (see for example Anderson and Minster, 1979). Therefore:

$$Z_I = -\frac{J\,l}{4\pi\,R}\frac{\eta_{\min}}{\eta_{\min} - \mu_M}\mu_{\text{M}} = \mu(2\omega_{\text{M}}) = -\sum_{k=2}^{\text{M}}\left(\frac{4\pi}{T_{\text{M}}}\right)^{k-1}p_{k-1} \tag{22}$$

The value μ_{M} represents the viscosity decrease at the frequency of Moon rotation with respect to the quasi-static value $\eta_{\min}$. The previous equations together with Eq. (20) provides:

$$\eta_{\min}(\eta_{\min}-\mu_M)=\frac{1}{8\pi T_M\omega_{Drift}}\left(\frac{Jl}{R}\right)^2\left(\frac{Gm\rho\, hT_M}{R^2}\right)^2 \quad (23)$$

We can use the numerical values:

$\omega_{Drift}\approx 10^{-16}$ rad/s, $\beta_1=\eta_{\min}=10^{14}$ Pa·s, $G=6.67\times10^{-11}$ Nm^2/kg^2, $m=7.34\times10^{22}$ kg, $\rho=4\times10^3$ kg/m^2, $R=3.84\times10^8$ m, $z_L=6.1\times10^6$ m, $z_0=10^6$ m, $r=6.36\times10^6$ m, $l=1.5\times10^5$ m, $h=10^4$ m, $T_M=8.6\times10^4$ s

With these values, the previous equation is solved for example for $\eta_{\min}\approx10^{13}$ Pa·s, $\eta_{\min}-\mu_M\approx10^9$ Pa·s. This formula provides a reference value of viscosity 10^{13} Pa·s that can be in agreement with recent estimates in the scientific literature (Scoppola et al., 2006) and uses a rheological model that triggers a decrease of viscosity with frequency.

The tidal oscillation mechanism described above, explains how the Moon gravitation can be responsible for a combined ratchet drift motion of the tectonic plates together with the known tidal oscillation and the misalignment of the tidal bulge generating a permanent westerly oriented torque. This result could identify Moon gravitation as one of the potential cause for both these effects. Note we demonstrate that, for an extremely large class of constitutive relationships characterizing the mantle response, the plate drift emerges due to a small nonlinear effect due to the Moon gravitation force.

A final comment on the value obtained for $\Delta\varphi_{Tidal}$ is useful. In fact, one obtains, for a large class of rheological models $\Delta\varphi_{Tidal}=\varepsilon|Z|=(Jl/4\pi R)\varepsilon$ and, since $\omega_{Drift}=1/8\pi((Jl/R)\varepsilon)^2\ 1/T_M\approx10^{-16}$ rad s^{-1}, it follows $\Delta\varphi_{Tidal}=\sqrt{\omega_{Drift}T_M/2\pi}\approx10^{-6}$ rad *i.e.* about 10 m of tidal wave displacement at the Earth's surface. Considering this value is for a single free-plate (considered as a point mass) without any lateral viscous-elastic constraint, it represents only an upper bound estimate. In fact, this value diminishes when considering, in a more realistic description, a system of interacting plates. In this case, each plate limits its oscillation due to the lateral force of its neighbors. This produces a decrease in the oscillation $\Delta\varphi_{Tidal}$, while the drift mechanism is less affected by this process. To qualitatively illustrate the point, consider the previous theory applied to a binary plate P1–P2 system, consisting of two point masses at initial angular distance $\Delta\psi$ and interacting by a viscous mechanism such that their interaction force is expressed by $\chi/2\left(\dot\varphi_1-\dot\varphi_2\right)$, where $\chi=2(\eta_{12}/\eta_{\min})$, and η_{12} is a viscosity related to the P1–P2 interaction. The perturbation solution for the two-plates takes the form (first index is to identify the plate, the second identifies the order of the perturbation and inertial force is neglected) $\varphi_1=\varphi_{10}+\varepsilon\varphi_{11}+\varepsilon^2\varphi_{12}$, $\varphi_2=\varphi_{20}+\varepsilon\varphi_{21}+\varepsilon^2\varphi_{22}$. Using an identical approach, as the one illustrated for the single free-plate, after some mathematics we find:

$$\begin{aligned}\omega_{Drift}&=\frac{1}{8\pi}\left(\frac{Jl}{R}\varepsilon\right)^2\frac{1}{T_M}\frac{1}{(1+2\chi)^2}\left(1+3\chi+2\chi^2+\chi\cos\Delta\psi+2\chi^2\cos\Delta\psi\right)\\ \Delta\varphi_{Tidal}&=\varepsilon|Z|=\frac{1}{4\pi}\frac{Jl}{R}\varepsilon\frac{1}{1+2\chi}\left(1+2\chi+2\chi^2+2\chi\cos\Delta\psi+2\chi^2\cos\Delta\psi\right)^{1/2}\end{aligned} \quad (24)$$

For example for $\chi\approx0.5$ and $\Delta\psi\approx35^\circ$, the tidal oscillation of the plate is reduced from 10 m to less than 5 m, with a comparable value of the viscosity and the same drift speed of the plate. This supports the idea that the mutual restraints between the point of the lithosphere, reduces the tidal oscillation and not proportionally the tidal drift. This theory can include a set of connected plates where their spacing is arbitrary and interaction forces are obtained by a generalized constitutive relationship.

4. Results

The developed theory suggests that any daily tidal oscillation due to the gravitation of the Moon, involves the ratchet drift process of the tectonic plates as a side effect. This is due to the geometric nonlinearity associated to the gravity that generates a ponderomotive drift force on moving particles over the Earth's surface. This effect works regardless the rheology of the mantle is linear or nonlinear. The order of magnitude of the drift angular speed of a tectonic plate under this action depends on the minimum viscosity in the low velocity layer and a value about $\eta_{min}\approx10^{13-15}$ Pa·s would permit a tectonic plate drift speed of about some centimeters per year.

5. Discussion and conclusions

Plate kinematics in the hotspot reference frame or relative to fixed Antarctica supports a "westerly" lithospheric net rotation relative to the underlying mantle. Two competing models have been proposed to explain this observation, (1) the uncompensated faster motion of the Pacific plate with respect to the other tectonic plates due to the slab pull at its western margin or (2) the tidal drag. The first model is at odds with the overestimation of the oceanic lithosphere negative buoyancy. The second model was discarded because the viscosity of the low-velocity layer was considered too high with respect to the values inferred to allow the decoupling. However, the Gutenberg-Richter law on the global frequency of earthquakes supports an Earth scale mechanism governing the tectonic energy dissipation, i.e., an astronomical tuning (Riguzzi et al., 2010). Here we have shown that the oscillating tidal drag exerted by the Moon is able to steadily shift the lithosphere relative to the underlying mantle allowing the decoupling of the lithosphere with the present inferred viscosity values of the low velocity layer. This nonlinear rheology derives from the asymmetry of the

gravitational traveling load when interacting with slowly moving bodies over the Earth's surface. Namely, the time the plates move in direction opposed to the Moon revolution is slightly shorter than the time they are pulled toward the Moon, producing a slow one-directional motion of the plates. A nonlinear phenomenon of symmetry breaking may induce the tidal ratchet that can explain the polarization of plate tectonics, supporting the astronomical tuning of plate motions and mantle convection under a permanent 'westerly' directed torque exerted by the tidal bulge misalignment (e.g., Doglioni and Panza, 2015; Cuffaro and Doglioni, 2017). Relative velocity between plates can be explained by average viscosity gradients in the LVZ planform controlled by the geochemistry, temperature and thickness of the low velocity layer (e.g., Chalot-Prat et al., 2017).

Acknowledgments

The study was supported by Sapienza University. Discussions with Don Anderson, Eugenio Carminati, Françoise Chalot-Prat, Marco Cuffaro, Eleonora Ficini, Corrado Mascia, Enzo Nesi, Diego Perugini, Alik Ismail-Zadeh, Giuliano Panza and Peter Varga were very fruitful. Sapienza University funded this research. The anonymous reviews and the Editorial Advisor M. Santosh are thanked for useful suggestions.

Appendix A. Supplementary data

Supplementary data related to this article can be found at https://doi.org/10.1016/j.gsf.2017.11.009.

References

Afonso, J.C., Fernandez, M., Ranalli, G., Griffin, W.L., Connolly, J.A.D., 2008. Integrated geophysical-petrological modeling of the lithosphere and sublithospheric upper mantle: methodology and applications. Geochemistry Geophysics Geosystems 9. https://doi.org/10.1029/2007GC001834. Q05008.

Anderson, D.L., Minster, J.B., 1979. The frequency dependence of Q in the Earth and implications for mantle rheology and Chandler wobble. Geophysical Journal of the Royal Astronomical Society 58, 431–440.

Anderson, D.L., 2011. Hawaii, boundary layers and ambient mantle–geophysical constraints. Journal of Petrology 52 (7-8), 1547–1577.

Bird, P., 2003. An updated digital model of plate boundaries. Geochemistry, Geophysics, Geosystems 4 (3). https://doi.org/10.1029/2001GC000252.

Bostrom, R.C., 1971. Westward displacement of the lithosphere. Nature 234, 356–538.

Cadek, O., van den Berg, A.P., 1998. Radial profiles of temperature and viscosity in the Earth's mantle inferred from the geoid and lateral seismic structure. Earth and Planetary Science Letters 164, 607–615.

Cathles, L.M., 1975. The Viscosity of the Earth's Mantle. Princeton University Press.

Chalot-Prat, F., Doglioni, C., Falloon, T., 2017. Westward migration of oceanic ridges and related asymmetric upper mantle differentiation. Lithos 268–271. https://doi.org/10.1016/j.lithos.2016.10.036, 163–173.

Crespi, M., Cuffaro, M., Doglioni, C., Giannone, F., Riguzzi, F., 2007. Space geodesy validation of the global lithospheric flow. Geophysical Journal International 168, 491–506.

Cruciani, C., Carminati, E., Doglioni, C., 2005. Slab dip vs. lithosphere age: no direct function. Earth and Planetary Science Letters 238, 298–310.

Cuffaro, M., Caputo, M., Doglioni, C., 2008. Plate sub-rotations. Tectonics 27. https://doi.org/10.1029/2007TC002182, 2008. TC4007.

Cuffaro, M., Doglioni, C., 2007. Global kinematics in the deep versus shallow hotspot reference frames. In: Foulger, G.R., Jurdy, D.M. (Eds.), Plates, Plumes, and Planetary Processes, Geological Society of America Special Paper 430, pp. 359–374.

Cuffaro, M., Doglioni, C., 2017. On the increasing size of the orogens moving from the Alps to the Himalayas in the frame of the net rotation of the lithosphere. Gondwana Research. https://doi.org/10.1016/j.gr.2017.09.008.

Doglioni, C., 1993. Geological evidence for a global tectonic polarity. Journal of the Geological Society of London 150, 991–1002.

Doglioni, C., Anderson, D.L., 2015. Top driven asymmetric mantle convection. In: Foulger, G.R., Lustrino, M., King, S.D. (Eds.), The Interdisciplinary Earth: A volume in honor of Don L. Anderson. Geological Society of America Special Paper 514. American Geophysical Union Special Publication 71. https://doi.org/10.1130/2015.2514(05).

Doglioni, C., Carminati, E., Cuffaro, M., Scrocca, D., 2007. Subduction kinematics and dynamic constraints. Earth-Science Reviews 83, 125–175.

Doglioni, C., Ismail-Zadeh, A., Panza, G., Riguzzi, F., 2011. Lithosphere-asthenosphere viscosity contrast and decoupling. Physics of the Earth and Planetary Interiors 189, 1–8.

Doglioni, C., Carminati, E., Crespi, M., Cuffaro, M., Penati, M., Riguzzi, F., 2015. Tectonically asymmetric Earth: from net rotation to polarized westward drift of the lithosphere. Geoscience Frontiers 6 (3), 401–418.

Doglioni, C., Green, D., Mongelli, F., 2005. On the shallow origin of hotspots and the westward drift of the lithosphere. In: Foulger, G.R., Natland, J.H., Presnall, D.C., Anderson, D.L. (Eds.), Plates, Plumes and Paradigms. Geological Society of America Special Paper 388, pp. 735–749.

Doglioni, C., Panza, G.F., 2015. Polarized plate tectonics. Advances in Geophysics 56 (3), 1–167. https://doi.org/10.1016/bs.agph.2014.12.001.

Elmore, W.C., Heald, M.A., 1969. Physics of Waves. Mc Graw Hill Book Company, New York.

Ficini, E., Dal Zilio, L., Doglioni, C., Gerya, T., 2017. Horizontal mantle flow controls subduction dynamics. Scientific Reports. https://doi.org/10.1038/s41598-017-06551-y.

Green, D.H., Hibberson, W.O., Kovacs, I., Rosenthal, A., 2010. Water and its influence on the lithosphere–asthenosphere boundary. Nature 467, 448–451.

Gripp, A.E., Gordon, R.G., 2002. Young tracks of hotspots and current plate velocities. Geophysical Journal International 150, 321–361.

Hansen, L.N., Zimmerman, M.E., Kohlstedt, D.L., 2012. Laboratory measurements of the viscous anisotropy of olivine aggregates. Nature 492 (7429), 415–418.

Hu, Y., Bürgmann, R., Banerjee, P., Feng, L., Hill, E.M., Ito, T., Tabei, T., Kelin Wang, K., 2016. Asthenosphere rheology inferred from observations of the 2012 Indian Ocean earthquake. Nature 538, 368–372.

Jin, Z.-M., Green, H.G., Zhou, Y., 1994. Melt topology in partially molten mantle peridotite during ductile deformation. Nature 372, 164–167.

Jordan, T.H., 1974. Some comments on tidal drag as a mechanism for driving plate motions. Journal of Geophysical Research 79 (14), 2141–2142.

Kohlstedt, D.L., Hansen, L.N., 2015. Constitutive equations, rheological behavior, and viscosity of rocks. Constitutive equations, rheological behavior, and viscosity of rocks. In: Schubert, Gerald (Ed.), Treatise on Geophysics, second ed., vol. 2. Elsevier, Oxford, pp. 441–472.

Leoncini, X., Neishtadt, A., Vasiliev, A., 2009. Directed transport in a spatially periodic harmonic potential under periodic nonbiased forcing. Physical Review E 79, 026213.

Le Pichon, X., 1968. Sea-floor spreading and continental drift. Journal of Geophysical Research 73 (12), 3661–3697.

Mainardi, F., Spada, G., 2011. Creep relaxation and viscosity properties for basic fractional models in rheology. The European Physical Journal 193 (1), 133–160.

Moore, G.W., 1973. Westward tidal lag as the driving force of plate tectonics. Geology 1, 99–100.

Naif, S., Key, K., Constable, S., Evans, R.L., 2013. Melt-rich channel observed at the lithosphere–asthenosphere boundary. Nature 495, 356–359.

Panza, G., Doglioni, C., Levshin, A., 2010. Asymmetric ocean basins. Geology 38, 59–62.

Pollitz, F.F., Burgmann, R., Romanowicz, B., 1998. Viscosity of oceanic asthenosphere inferred from remote triggering of earthquakes. Science 280, 1245–1249.

Ranalli, G., 2000. Westward drift of the lithosphere: not a result of rotational drag. Geophysical Journal International 141, 535–537.

Reimann, P., 2002. Brownian motors: noisy transport far from equilibrium. Physics Reports 361, 57–265.

Ricard, Y., Doglioni, C., Sabadini, R., 1991. Differential rotation between lithosphere and mantle: a consequence of lateral viscosity variations. Journal of Geophysical Research 96, 8407–8415.

Riguzzi, F., Panza, G., Varga, P., Doglioni, C., 2010. Can Earth's rotation and tidal despinning drive plate tectonics? Tectonophysics 484, 60–73.

Rychert, C.A., Fischer, C.M., Rondenay, S., 2005. A sharp lithosphere–asthenosphere boundary imaged beneath eastern North America. Nature 436, 542–545.

Rychert, C.A., Laske, G., Harmon, N., Shearer, P.M., 2013. Seismic imaging of melt in a displaced Hawaiian plume. Nature Geoscience 6 (8), 657–660.

Schmerr, N., 2012. The Gutenberg discontinuity: melt at the lithosphere-asthenosphere boundary. Science 335, 1480–1483.

Scoppola, B., Boccaletti, D., Bevis, M., Carminati, E., Doglioni, C., 2006. The westward drift of the lithosphere: a rotational drag? Bulletin of the Geological Society of America 118, 199–209.

Torsvik, T.H., Steinberger, B., Gurnis, M., Gaina, C., 2010. Plate tectonics and net lithosphere rotation over the past 150 Myr. Earth and Planetary Science Letters 291, 106–112.

van Keken, P.E., Bradley, R.H., Syracuse, E.M., Abers, G.A., 2011. Subduction factory: 4. Depth-dependent flux of H_2O from subducting slabs worldwide. Journal of Geophysical Research 116, B01401.

Antonio Carcaterra is full professor at Sapienza University in Rome, Italy, at the Department of Mechanical and Aerospace Engineering. He is the President of Sapienza Innovation, Director of the Master Inventive Engineering and in charge of the Laboratory of Vehicle Dynamics and Mechatronics. He has been Adjunct Professor from 2006 to 2010 at the Department of Mechanical Engineering at Carnegie Mellon University, USA. He is Coordinator of the PhD program in Theoretical and Applied Mechanics. His current scientific interests are structural dynamics, vibrations, acoustics, vehicle dynamics, micro/nano systems, damping and dissipation.

Carlo Doglioni is full professor at Sapienza University in Rome, Italy, at the Department of Earth Sciences and is currently President of the Italian Geophysical and Volcanological Institute. His scientific interests are the mechanisms of plate tectonics, the earthquake dynamics, the structure and evolution of orogens and subduction zones. He is member of the National Academy of Lincei, Academy of Sciences XL, the Academy of Europe and several other institutions.

e-component SUPPLEMENTARY information

The westward drift of the lithosphere: a tidal ratchet?

A. Carcaterra and C. Doglioni

Detailed mathematics of the paper

1. Bulk and effective viscosity

We want to compare the two cases of figure 2. In the absence of any horizontal force along z we have (using notation from the mathematics of the paper):

$$\frac{\partial}{\partial z}\left[A\eta(z)\dot{\gamma}_{xz}\right]=0,\quad A\eta(z)\frac{\partial v_x}{\partial z}=\alpha,\quad \frac{\partial v_x}{\partial z}=\frac{\alpha}{A\eta(z)},\quad v_x(z)=\frac{\alpha}{A}\int_{z_0}^{z}\frac{dz'}{\eta(z')}++v_x(z_0)\approx\frac{\alpha}{A}\frac{z-z_0}{\eta_{bulk}}+v_x(z_0)$$

For a constant bulk viscosity, we have:

$$\int_{z_0}^{z}\frac{dz'}{\eta(z')}\approx\frac{z-z_0}{\eta_{bulk}}=\frac{z-z_0}{\overline{\eta}}$$

In the presence of the LVZ, we have and comparing with the above:

$$\int_{z_0}^{z}\frac{dz'}{\eta(z')}\approx\frac{l}{\eta_{min}}=\frac{z-z_0}{\eta_{eff}}$$

deducing $\eta_{eff}=\eta_{min}\frac{z-z_0}{l}=\eta_{min}\frac{h_0}{l}$.

2. The perturbation expansion for the single plate

We provides details for the perturbation solution to equation:

$$\Pi\sum_{k=0}^{N}\frac{\alpha_k}{T_M^k}\frac{d^{k+2}\varphi(\tau)}{d\tau^{k+2}}+\sum_{k=1}^{M}\frac{\beta_k/\beta_{1min}}{T_M^{k-1}}\frac{d^k\varphi(\tau)}{d\tau^k}=\varepsilon\frac{l}{R}J\sum_{k=0}^{N}\frac{\alpha_k}{T_M^k}\frac{d^k}{d\tau^k}\sin(4\pi\tau-2\varphi) \qquad \text{(S1)}$$

where $\varepsilon=\frac{f_0T_M}{A\beta_{1\min}}$, $\Pi=2\frac{\rho hl}{\beta_{1min}T_M}$. The physical key to determine φ form (S1) relies on the chance to examine the plate motion when the plate rotation φ is small with respect to the Moon's one $\omega_M t$.

This means we are interested in solutions for which $|\varphi| << \omega_M t$ or $\frac{|\dot{\varphi}|}{\omega_M} << 1$. The dimensionless parameter $\varepsilon = \frac{f_0 T_M}{A\beta_{1\min}}$ controls the overall speed $|\dot{\varphi}|$ of the plate. In fact, considering f_0 as a constant amplitude tidal driving force, the steady state speed of the plate under this force is simply $\frac{f_0}{A\beta_{1\min}}$, that implies the dimensionless parameter ε verifies the inequality $\frac{f_0}{A\beta_{1\min}\omega_M} = \frac{1}{2\pi}\frac{f_0 T_M}{A\beta_{1\min}} = \frac{1}{2\pi}\varepsilon << 1$ for the condition $|\varphi| << \omega_M t$ to hold.

This makes it possible to use a perturbation expansion $\varphi = \varphi_0 + \varepsilon\varphi_1 + \varepsilon^2\varphi_2 + ...$ for the plate motion, where the φ_k will be determined in analytical form, revealing the presence of an oscillatory motion at a lower order, and a drift motion at a higher order. Using a Taylor series up to the first order for ε, the trigonometric term in equation (S1) becomes:

$$\sin\left(4\pi\tau - 2\varphi_0 - 2\varepsilon\varphi_1 - 2\varepsilon^2\varphi_2\right) \approx \sin\left(4\pi\tau - 2\varphi_0\right) - 2\varepsilon\varphi_1\cos\left(4\pi\tau - 2\varphi_0\right)$$

that makes the RHS of equation (S1) second order with respect to ε, consistently with the used order of the expansion for φ:

$$\Pi\sum_{k=0}^{N}\frac{\alpha_k}{T_M^k}\frac{d^{k+2}\varphi(\tau)}{d\tau^{k+2}} + \sum_{k=1}^{M}\frac{\beta_k/\beta_{1\min}}{T_M^{k-1}}\frac{d^k\varphi(\tau)}{d\tau^k} = J\frac{l}{R}\sum_{k=0}^{N}\frac{\alpha_k}{T_M^k}\frac{d^k}{d\tau^k}\left[\varepsilon\sin\left(4\pi\tau - 2\varphi_0\right) - 2\varepsilon^2\varphi_1\cos\left(4\pi\tau - 2\varphi_0\right)\right] \quad \text{(S2)}$$

Therefore, we identify two different amplitude scales for the force as ε, ε^2, and we can use the perturbation expansion $\varphi = \varphi_0 + \varepsilon\varphi_1 + \varepsilon^2\varphi_2$, to follow the response at each scale, yielding the cascade:

$$\begin{cases} \Pi\sum_{k=0}^{N}\frac{\alpha_k}{T_M^k}\frac{d^{k+2}\varphi_0}{d\tau^{k+2}} + \sum_{k=1}^{M}\frac{\beta_k/\beta_{1\min}}{T_M^{k-1}}\frac{d^k\varphi_0}{d\tau^k} = 0 \\ \Pi\sum_{k=0}^{N}\frac{\alpha_k}{T_M^k}\frac{d^{k+2}\varphi_1}{d\tau^{k+2}} + \sum_{k=1}^{M}\frac{\beta_k/\beta_{1\min}}{T_M^{k-1}}\frac{d^k\varphi_1}{d\tau^k} = J\frac{l}{R}\sum_{k=0}^{N}\frac{\alpha_k}{T_M^k}\frac{d^k}{d\tau^k}\sin\left(4\pi\tau - 2\varphi_0\right) \\ \Pi\sum_{k=0}^{N}\frac{\alpha_k}{T_M^k}\frac{d^{k+2}\varphi_2}{d\tau^{k+2}} + \sum_{k=1}^{M}\frac{\beta_k/\beta_{1\min}}{T_M^{k-1}}\frac{d^k\varphi_2}{d\tau^k} = -2J\frac{l}{R}\sum_{k=0}^{N}\frac{\alpha_k}{T_M^k}\frac{d^k}{d\tau^k}\left[\varphi_1\cos\left(4\pi\tau - 2\varphi_0\right)\right] \end{cases}$$

Considering only the asymptotic plate response in the long time, i.e. neglecting any transient, from the first equation we obtain $\varphi_0 = 0$. First order solution φ_1, under the same hypothesis, is purely harmonic, and the oscillation of the plate is determined as $\varphi_1 = \mathcal{I}m\left\{Z e^{4\pi j\tau}\right\}$ in response to the RHS dimensionless force $J\frac{l}{R}\sum_{k=0}^{N}\frac{\alpha_k}{T_M^k}\frac{d^k}{d\tau^k}\mathcal{I}m\left\{e^{4\pi j\tau}\right\}$. Substituting into the first order equation, we obtain:

$$Z = Z_R + jZ_I = J\frac{l}{R}\frac{\sum_{k=0}^{N}\frac{\alpha_k}{T_M^k}(4\pi j)^k}{\Pi\sum_{k=0}^{N}\frac{\alpha_k}{T_M^k}(4\pi j)^{k+2} + \sum_{k=1}^{M}\frac{\beta_k/\beta_{1\min}}{T_M^{k-1}}(4\pi j)^k} \quad \text{(S3)}$$

That provides the first order harmonic solution, at frequency $2\omega_M$.

Physically, expression (S3), corresponds to the major contribution (order ε) to the daily tidal oscillation $\varphi_1 = \mathrm{Im}\left\{\left(Z_R + jZ_I\right)\left(\cos 4\pi\tau + j\sin 4\pi\tau\right)\right\} = Z_I\cos 4\pi\tau + Z_R\sin 4\pi\tau$, of amplitude $|Z|$.

The force term of the second order equation is:

$$-2J\frac{l}{R}\sum_{k=0}^{N}\frac{\alpha_k}{T_M^k}\frac{d^k}{d\tau^k}\left[\varphi_1\cos\left(4\pi\tau-2\varphi_0\right)\right] = -2J\frac{l}{R}\sum_{k=0}^{N}\frac{\alpha_k}{T_M^k}\frac{d^k}{d\tau^k}\left[\left(Z_I\cos 4\pi\tau + Z_R\sin 4\pi\tau\right)\cos\left(4\pi\tau\right)\right]$$

The only drift generated on the RHS force is the constant term $-J\frac{l}{R}Z_I$ (derived from cosine square), all the others are indeed harmonic at frequency $4\omega_M$, and smaller with respect to those generated by the first order term solution.

Therefore, the complete physically significant solution to the plate equation of motion is:

$$\varphi(\tau) = \varepsilon\varphi_1(\tau) + \varepsilon^2\varphi_2(\tau) = \varepsilon\left(Z_I\cos 4\pi\tau + Z_R\sin 4\pi\tau\right) - \varepsilon^2 J\frac{l}{R}Z_I\tau \qquad \text{(S4)}$$

3. The perturbation expansion for two coupled plates

Considering this value is for a single free-plate (as a point mass) without any lateral viscous-elastic constraint, it represents only an upper bound estimate. In fact, this value diminishes when considering a system of interacting plates, in a more realistic description. In this case, each plate limits its oscillation due to the lateral force of its neighbors. This produces a decrease in the oscillation $\Delta\varphi_{Tidal}$, while the drift mechanism is less affected by this process. To qualitatively illustrate the point, consider the previous theory applied to a binary plate P1-P2 system, consisting of two point masses at initial angular distance $\Delta\psi$ and interacting by a viscous mechanism such that their interaction force is expressed by $\frac{\chi}{2}\left(\varphi_1-\varphi_2\right)$, where $\chi = 2\frac{\eta_{12}}{\eta_{min}}$, and η_{12} is a viscosity related to the P1-P2 interaction. The previous perturbation equation for the two-plates takes the form (first index is to identify the plate, the second identifies the order of the perturbation and inertial force is neglected):

$$\begin{cases} \dfrac{d\varphi_{10}}{d\tau} = 0,\ \dfrac{d\varphi_{20}}{d\tau} = 0 \\ \dfrac{d\varphi_{11}}{d\tau} + \chi\dfrac{d}{d\tau}\left(\varphi_{11}-\varphi_{21}\right) = J\dfrac{l}{R}\sin\left(2\varphi_{10}-4\pi\tau\right),\ \dfrac{d\varphi_{21}}{d\tau} + \chi\dfrac{d}{d\tau}\left(\varphi_{21}-\varphi_{11}\right) = J\dfrac{l}{R}\sin\left(2\varphi_{20}-4\pi\tau-\Delta\psi\right) \\ \dfrac{d\varphi_{12}}{d\tau} + \chi\dfrac{d}{d\tau}\left(\varphi_{12}-\varphi_{22}\right) = J\dfrac{l}{R}\varphi_{11}\cos\left(2\varphi_{10}-4\pi\tau\right),\ \dfrac{d\varphi_{22}}{d\tau} + \chi\dfrac{d}{d\tau}\left(\varphi_{22}-\varphi_{12}\right) = J\dfrac{l}{R}\varphi_{21}\cos\left(2\varphi_{20}-4\pi\tau-\Delta\psi\right) \end{cases}$$

where we use $\varphi_1 = \varphi_{10} + \varepsilon\varphi_{11} + \varepsilon^2\varphi_{12}$, $\varphi_2 = \varphi_{20} + \varepsilon\varphi_{21} + \varepsilon^2\varphi_{22}$.